Mikailalsys Journal of Mathematics and Statistics

e-ISSN : 3030-816X
p-ISSN : 3030-8399

Index : Harvard, Boston, Sydney University, Dimensions, Lens, Scilit, Semantic, Google, etc

https://doi.org/10.58578/MJMS.v4i1.7658

Development of a Predictor-Corrector Algorithm for the Numerical Solution of the Time-Fractional Vibration Equation

Falade Kazeem Iyanda[1], Dauda Alani Dikko[2], Adeyemo Kolawole Adefemi[3], Adepoju Ajibola Akeem[4], Muhammad Yusuf Muhammad[5], Shehu Jemilu[6]

[1,4,5,6]Aliko Dangote University of Science and Technology, Wudil Kano State, Nigeria

[2]University of Ibadan, Oyo State, Nigeria; [3]Nigeria Police Academy, Wudil Kano State Nigeria

faladekazeem2016@kustwudil.edu.ng; da.dikko@mail.ui.edu.ng

Article Info:

Submitted:	Revised:	Accepted:	Published:
Oct 7, 2025	Oct 30, 2025	Nov 12, 2025	Nov 17, 2025

Abstract

This study employs a predictor–corrector approach to solve the time-fractional vibration equation governing the transverse deflection of a cable of length L fixed at both ends. The model incorporates the Riemann–Liouville time-fractional derivative to accurately represent memory effects and damping behavior characteristic of composite and viscoelastic materials. Spatial discretization is performed using a finite difference method, while the temporal fractional derivative is approximated through a carefully formulated predictor–corrector scheme. This technique effectively addresses the initial conditions and captures the nonlocal temporal dynamics introduced by the fractional derivative. Numerical experiments demonstrate that the proposed method is accurate, stable, and computationally efficient in simulating damped vibrations in elastic and composite cables. By offering a reliable numerical framework, the approach enables more precise analysis of vibrating systems with memory effects and material heterogeneity, thereby contributing to improved modeling

MJMS Journal is licensed under a Creative Commons Attribution-NonCommercial-ShareAlike 4.0 International License

and design in engineering applications involving time-dependent mechanical behavior.

Keywords: Time-Fractional Vibration Equation; Riemann–Liouville Derivative; Predictor–Corrector Method; Finite Difference Scheme; Viscoelastic Materials

Introduction

Modeling dynamic systems with memory and hereditary effects has garnered a lot of interest lately, particularly when it comes to viscoelastic and composite materials. Such complicated dynamics are frequently not adequately captured by conventional vibration models that rely on classical integer-order derivatives. Fractional calculus has become an effective mathematical technique to overcome this constraint, enabling the extension of derivatives to non-integer orders. Time-fractional partial differential equations (PDEs) have shown remarkable success in simulating systems with anomalous dynamic responses, damping, and long-term memory. Such models are widely used in the investigation of transverse vibrations in flexible cables and beams that are exposed to bending stiffness and axial strain. A more accurate depiction of the energy dissipation and damping mechanisms found in composite or viscoelastic materials is offered by the governing equation, which incorporates a Caputo time-fractional derivative. The time-fractional vibration equation of interest because fractional derivatives are nonlocal, it is frequently impossible to solve them analytically. Therefore, reliable and effective numerical techniques are crucial. The predictor-corrector algorithm structure for the time-fractional vibration equation and the approach combines the approximation for the time-fractional Caputo derivative with spatial discretization techniques based on finite differences. The predictor-corrector technique is appropriate for complicated structural analysis because it improves accuracy and stability. Numerical experiments confirm the approach and show that it can predict fractional dynamic behavior in engineering structures.

A cable of length L that is fixed at both ends has a transverse deflection $\Phi(x, t)$, which is determined by the time-fractional vibration equation discussed in this article. The Caputo time-fractional derivative is used in the model to take memory effects and damping behavior in composite and viscoelastic structures into consideration of the form:

$$\frac{\partial^{\alpha}\Phi(\mathrm{x},\mathrm{t})}{\partial t^{\alpha}} = -R\frac{\partial^{4}\Phi(\mathrm{x},\mathrm{t})}{\partial x^{4}} + T\frac{\partial^{2}\Phi(\mathrm{x},\mathrm{t})}{\partial x^{2}} + \mathrm{q}(\mathrm{x},\mathrm{t}), \quad 0 < \alpha \leq 1 \qquad (1)$$

The initial shape (deflection) and the rate of change (velocity) at $t = 0$ are given as:

$$\begin{cases} \Phi(\mathrm{x},0) = \psi(x), \\ \left.\dfrac{\partial\Phi(\mathrm{x},\mathrm{t})}{\partial t}\right|_{t=0} = \vartheta(x), \end{cases} \qquad (2)$$

Where T denotes the axial tension, R represents the flexural stiffness, and $\mathrm{q}(\mathrm{x},\mathrm{t})$ is a distributed transverse load. The relationship between axial tension$T$, flexural stiffness R, and the distributed transverse load $\mathrm{q}(\mathrm{x},\mathrm{t})$arises from the mechanical behavior of a cable or beam undergoing transverse vibration.

In recent years, several authors have worked on time-fractional vibration model such as [1] applied an efficient analytical technique for fractional model of vibration equation, [2] presented approximate solution of fractional vibration equation using Jacobi polynomials, [3] used Jacobi polynomials method to solve fractional vibration equation, [4] presented residual power series method for solving time-fractional model of vibration equation of large membranes, [5] fractional treatment of vibration equation through modern analogy of fractional differentiations using integral transforms, [6] presented a novel analytical iterative approach to time-fractional vibration equation, [7] presented solution of the vibration equation of large membranes in uncertain environment, [8] proposed the operational matrix approach for solving fractional vibration equation of large membranes with error estimation, [9] proposed a numerical approach for solving optimal control problem of fractional order vibration equation of large membranes,[10] presented numerical solutions of the time-delay fractional vibration resonance boosted weak fault detection of machinery, [11] numerical simulations and approximation using a classical Fractional Kelvin–Voigt model for beam vibrations, and [12] used cardinal-based approximate method for time fractional forced vibration analysis of Euler–Bernoulli viscoelastic beam.

Fractional Calculus [13]

Definition 1.Let $\alpha > 0$ we define the Riemann-Liouville fractional integral by

$$ {}_{0}^{R}D_{t}^{-\alpha}\Phi(x,t) = \frac{1}{\Gamma(\alpha)}\int_{0}^{t}(t-\tau)^{\alpha-1}\Phi(x,\tau)\,d\tau, \qquad \alpha > 0 \qquad (3) $$

Suppose $\alpha = 1$, then equation (2) reduces to the integral of the form

$$ {}_{0}^{R}D_{t}^{-1}\Phi(x,t) = \int_{0}^{t}\Phi(x,\tau)\,d\tau \qquad \alpha = 1 \qquad (4) $$

Definition 2. The fractional derivative in Caputo's sense is defined as

$$ {}_{0}^{R}D_{t}^{-\alpha}\Phi(x,t) = \frac{1}{\Gamma(n-\alpha)}\int_{0}^{t}(t-\tau)^{n-\alpha-1}\Phi^{(n)}(x,\tau)\,d\tau \qquad (5) $$

$n-1 < \alpha \leq n,\ \ n \in \mathbb{N}, t > 0$ provided the right-hand side exists.

Description of the predictor-corrector algorithm.

This algorithm discretizes the temporal domain using uniform time steps and the spatial domain using finite difference approximations. The system, which incorporates contributions from all prior time levels and reflects the memory effect, approximates the Caputo derivative. In the predictor step, an explicit estimate Φ_i^n at each spatial point is calculated using known values from previous steps. In the corrector step, this predicted value is refined using a trapezoidal rule, yielding a more accurate solution Φ_i^n. Spatial derivatives $\frac{\partial^2\Phi(x,t)}{\partial x^2}$ and $\frac{\partial^4\Phi(x,t)}{\partial x^4}$ are approximated using central difference formulas.At each time step, the initial and boundary conditions are applied to guarantee the cable's physical restrictions, such as fixed ends. Stepwise in time, the algorithm captures the system's dynamic response as it is affected by fractional damping, external loading, bending stiffness, tension, and the approach is reliable for modeling realistic vibration behavior in engineering structures.

Step 1: Discretization

Suppose the space domain is divided $[0, L]$is divided into M segments, with spacing $h = \frac{L}{M}$, the grid points are defined as $x_1 = ih$, for $i = 0,1, \ldots, M$. The time domain is divided $[0, L]$ into M steps, with the spacing τ.The time level $t_n = n\tau$, for $n = 0,1, \ldots, N$.

Let $\Phi_i^n \approx \Phi(x_i, t_n)$ (6)

Step 2: Caputo Fractional Derivative Approximation (Scheme)

The Caputo derivative of order $\alpha \in (0,1]$ at the t_n is approximated as

$$\frac{\partial^{\alpha}\Phi(t_n)}{\partial t^{\alpha}} \approx \frac{1}{\tau^{\alpha}\Gamma(2-\alpha)}\left(\Phi_i^n - \sum_{k=0}^{n-1} c_k^{(\alpha)} \Phi_i^{n-1-k}\right), \tag{7}$$

Where $c_k^{(\alpha)} = (k+1)^{1-\alpha} - k^{1-\alpha}$

Step 3: Spatial Derivative (Finite Difference Approximation)

Obtain the second derivative:

$$\left.\frac{\partial^2\Phi}{\partial x^2}\right|_{x_i} \approx \frac{\Phi_{i+1}^n - 2\Phi_i^n + \Phi_{i-1}^n}{h^2} \tag{8}$$

Fourth derivative:

$$\left.\frac{\partial^4\Phi}{\partial x^4}\right|_{x_i} \approx \frac{\Phi_{i-2}^n - 4\Phi_{i-1}^n + 6\Phi_i^n - 4\Phi_{i+1}^n + \Phi_{i+2}^n}{h^4} \tag{9}$$

Step 4: Predictor-Corrector Algorithm

Set the initial conditions:

$$\Phi_i^0 = \psi(x_i), \quad \left.\frac{\partial\Phi}{\partial t}\right|_{t=0} = \vartheta(x) \tag{10}$$

Using the Taylor expansion to estimate Φ_i^1, we obtain $\Phi_i^1 = \Phi_i^0 + \tau\vartheta(x)$

The explicit estimate is given as $\widehat{\Phi_i^n}$ using the unknown values from previous time steps:

$$\widehat{\Phi_i^n} = \Phi_i^0 + \frac{\tau^{\alpha}}{\Gamma(\alpha+1)}\sum_{k=0}^{n-1}(t_n - t_k)^{\alpha-1} F_i^k \tag{11}$$

Where:

$$F_i^k = -R\left.\frac{\partial^4\Phi}{\partial x^4}\right|_{x_i} + T\left.\frac{\partial^2\Phi}{\partial x^2}\right|_{x_i} + q(x_i, t_k)$$

The correct predicted value using the trapezoidal rule is given as

$$\Phi_i^n = \Phi_i^0 + \frac{\tau^{\alpha}}{\Gamma(\alpha+2)}\left[F_i^m + \sum_{k=0}^{n-1} b_{n-k-1} F_i^k\right] \tag{12}$$

Where the coefficients are:

$$b_k = (k+1)^{\alpha+1} - 2(k)^{\alpha+1} + (k-1)^{\alpha+1}$$

For a fixed beam or cable with clamped ends, obtained

$$\Phi_0^n = \Phi_M^n = 0, \quad \Phi_x(0,t) = \Phi_x(L,t) = 0 \tag{13}$$

The slope condition can be enforced using ghost points or symmetric approximations:

$$\Phi_{-1}^n = \Phi_1^n, \qquad \Phi_{M+1}^n = -\Phi_{M-1}^n \tag{14}$$

Repeat the procedures and advance to the time step $n = 1, \ldots, N$ and update Φ_i^n using the predictor steps.

Step 5: Display the output of the simulations in visualized 2D, 3D surfaces, and appendices.

Table 1. The outline of the predictor-corrector algorithm

Step	Description	Mathematical Expression
1. Discretization	Divide spatial domain $[0, L]$ into M segments of size $h = L/M$. Time domain $[0, T]$ into steps of size τ. Grid points: $x_i = ih$, $t_n = n\tau$.	$\Phi_i^n \approx \Phi(x_i, t_n)$
2. Caputo Fractional Derivative Approximation	Approximate the Caputo derivative of order $\alpha \in (0,1]$ at time t_n.	$\frac{\partial^\alpha \Phi(t_n)}{\partial t^\alpha} \approx \frac{1}{\tau^\alpha \Gamma(2-\alpha)} \left(\Phi_i^n - \sum_{k=0}^{n-1} c_k^{(\alpha)} \Phi_i^n$ where $c_k^{(\alpha)} = (k+1)^{1-\alpha} - k^{1-\alpha}$
3. Spatial Derivative Approximation	Use finite difference to approximate second and fourth spatial derivatives.	(\left. \frac{\partial^2 \Phi}{\partial x^2} \righ
4. Predictor-Corrector Algorithm	**Initial Conditions:** (\Phi_i^0 = \psi(x_i), \left. \frac{\partial \Phi}{\partial t} \right	_{t=0} = \vartheta(x_i)) **First step using Taylor expansion:** $\Phi_i^1 = \Phi_i^0 + \tau \vartheta(x_i)$ **Predictor (explicit):** Estimate $\hat{\Phi}_i^n$ using previous time steps: $\hat{\Phi}_i^n = \Phi_i^0 + \frac{\tau^\alpha}{\Gamma(\alpha+1)} \sum_{k=0}^{n-1} (t_n - t_k)^{\alpha-1} F_i^k$ **Corrector (implicit):** Refine prediction using trapezoidal rule: $\Phi_i^n = \Phi_i^0 + \frac{\tau^\alpha}{\Gamma(\alpha+2)} \left(F_i^n + \sum_{k=0}^{n-1} b_{n-k-1} F$
5. Boundary Conditions	Fixed (clamped) ends: $\Phi_0^n = \Phi_M^n = 0$, $\Phi_x(0,t) = \Phi_x(L,t) = 0$ **Symmetric/Ghost points:** $\Phi_{-1}^n = \Phi_1^n$, $\Phi_{M+1}^n = -\Phi_{M-1}^n$	
6. Time Marching	Repeat Steps 2–5 for $n = 1 \to N$ to update Φ_i^n	—

Error, Stability Analysis, and Convergence

Error

Error analysis in the fractional vibration equation using the predictor-corrector algorithm highlights the combined effects of the distributed transverse loadq(x, t), the axial tension T, the flexural stiffness T, fractional order memory effects, spatial approximation, and fractional derivative discretization. Error analysis of the described predictor-corrector technique requires an understanding of the truncation and approximation errors introduced at each discretization stage. Equation (7) exhibits global truncation error of order of the following type for the Caputo derivative approximation:

$$\mathcal{O}(\tau^{2-\alpha}) \qquad (15)$$

The coefficients $c_k^{(\alpha)}$ capture the memory effect of fractional derivatives, but still introduce approximation errors, especially for small α.

The spatial error of the second derivative of equation (8) has a truncation error of the order.

$$\mathcal{O}(h^2) \qquad (16)$$

The fourth derivative of the equation (9) has a truncation error of order

$$\mathcal{O}(h^4) \qquad (17)$$

Hence, the spatial accuracy depends on the smoothness of $\Phi(x, t)$.

Finally, the predictor equation (11) introduces an error of order

$$\mathcal{O}(\tau^{\alpha}) \qquad (18)$$

And the corrector equation (12) improves the accuracy using the trapezoidal rule, which reduces the local error to

$$\mathcal{O}(\tau^{\alpha+1}) \qquad (19)$$

Stability Analysis

The stability analysis determines if numerical errors improve over time. For the proposed predictor-corrector technique applied to a time-fractional vibration equation, we focus on the spatial derivative equation (8–9) and the Caputo derivative approximation (7). Every new value Φ_i^n is dependent on all previous times through the weighted coefficient

$c_k^{(\alpha)}$due to the memory introduced by the Caputa term. These coefficients contribute to algorithm stability by declining for$0 < \alpha < 1$. A trial solution of the following type is assumed using von Neumann stability analysis:

$$G^m e^{i\beta x_l} \qquad (20)$$

Where the amplification factor is denoted by G. It is evident that stability requires $|G| < 1$ when substituting into the scheme. For the predictor equation (11) and corrector equation (12) steps, stability is enhanced with small step sizes $\tau, h,$ coefficients $b_k,$ and a smooth source term $q(x, t)$. The algorithm method is therefore conditionally stable, relying on the physical parameters R and T as well as$\tau, h,$and α.

Convergence

The algorithm's convergence depends on stable fractional derivative approximation and consistent discretization of time and space. We approximate $\Phi_i^n \approx \Phi(x_i, t_n)$by discretizing the spatial domain $x_i = ih,\ i = 0,1,.,M$ and the time domain$t_n = n\tau,\ n = 0,1,\ldots,N$. An approximation of the Caputo derivative is

$$\frac{\partial^\alpha \Phi(t_n)}{\partial t^\alpha} \approx \frac{1}{\tau^\alpha \Gamma(2-\alpha)}\left(\Phi_i^n - \sum_{k=0}^{n-1} c_k^{(\alpha)} \Phi_i^{n-1-k}\right), \qquad (21)$$

With $c_k^{(\alpha)} = (k+1)^{1-\alpha} - k^{1-\alpha}$. The predictor-corrector scheme utilizes the previous solution to predict Φ_i^nequation (11), then corrects using a trapezoidal rule in equation (12). The convergence is guaranteed when the time step $\tau \to 0$ and the space $h \to 0$, and the stability condition are satisfied. The global error decays as$\mathcal{O}(\tau^\alpha + h^2)$, ensuring accurate solutions over time.

Numerical Computation

In this section, we apply the proposed predictor-corrector algorithm for the simulation solutions of the variation of $\alpha,$ the axial tension T, the flexural stiffness R, and $q(x, t)$the distributed transverse load.

Table 2. Suitable values for the experimental parameters

Symbol	Physical Meaning	Typical Numerical Value	Units	Interpretation
α	Fractional order of the time derivative	[0.2, 0.4, 0.6, 0.8,]		Controls memory effect in vibration
T	Axial tension	1000	N	Could be computed from
R	Flexural stiffness	$1.0X10^{-2}$	NM^2	Uniform beam
$q(x,t)$	Distributed transverse load	$10\sin(\pi x)\sin(\omega t)$	N/m	Harmonic forcing
$\Phi(x,t)$	Initial deflection shape	$sin\left(\frac{\pi x}{\omega}\right)$	m	First mode shape
$\frac{\partial\Phi(x,t)}{\partial t}\Big\vert_{t=0}$	Initial transverse velocity	0	m/s	Cable start from rest

We consider the initial deflection $\Phi(x,t)$, which describes the starting shape of the cable or beam before vibration begins, and initial transverse velocity $\frac{\partial\Phi(x,t)}{\partial t}\Big|_{t=0}$ describes the initial rate of change of the deflection of the form:

Initial displacement:

$$\Phi(x,0) = sin\left(\frac{\pi x}{\omega}\right) \tag{22}$$

Initial velocity:

$$\frac{\partial\Phi(x,t)}{\partial t}\Big|_{t=0} = 0 \tag{23}$$

The computational assessment of the ω forcing angular frequency, which describes how that mode oscillates in time and controls how rapidly the external load changes in time, was considered for simulation. The numerical results are presented in 2D and 3D plots. The higher the value of ω, the more vibration frequencies are recorded.

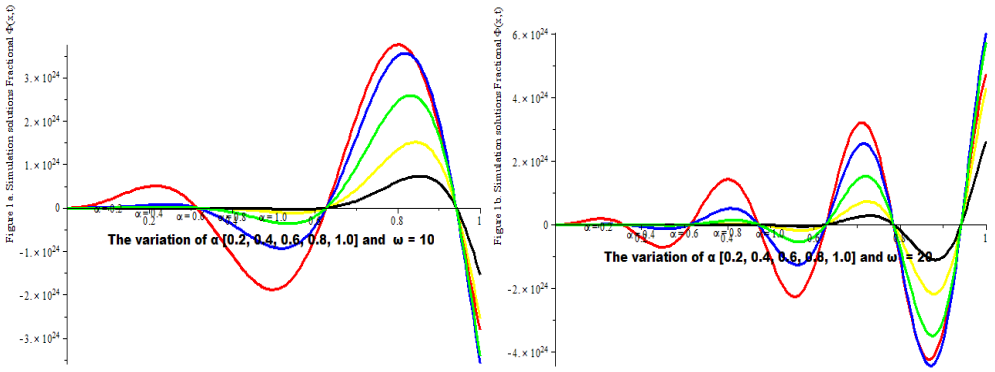

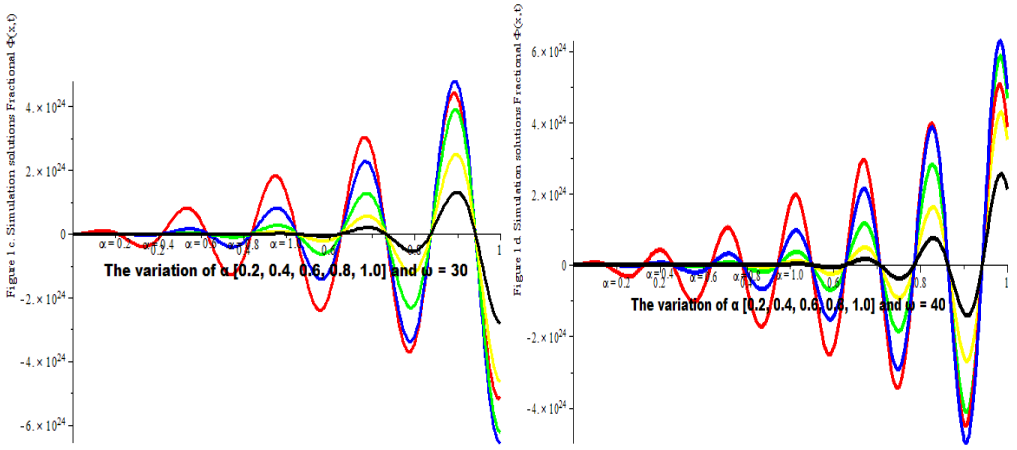

Fig. 1a.1b, 1c, 1d. Depict the trend of the deflection $\Phi(t)$ obtained for the various fractional derivatives and the assessment of $\omega = [10, 20, 30, 40]$ forcing angular frequency, which describes how that mode oscillates in time and controls how rapidly the external load changes in time.

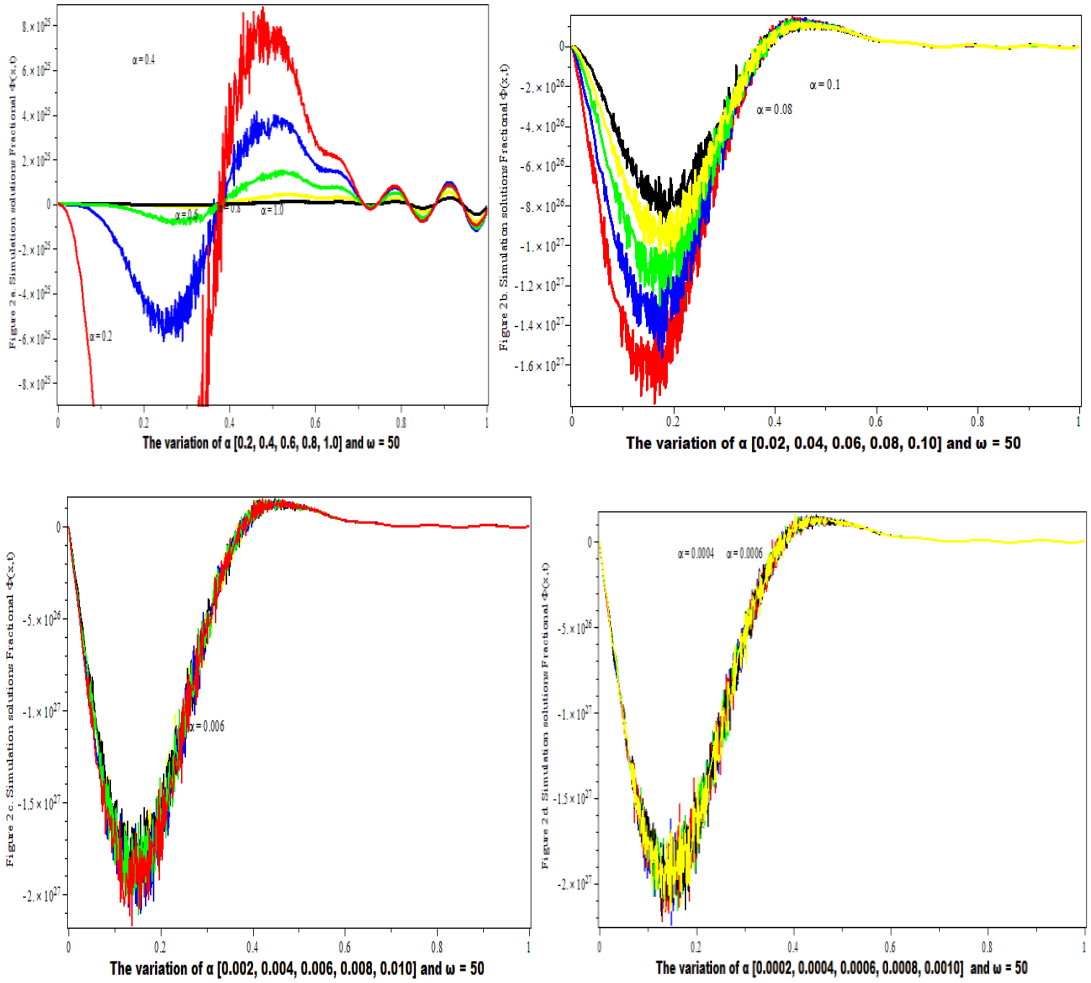

Fig. 2a.2b, 2c, 2d. Depict the trend of the deflection $\Phi(t)$ and amplitude frequency obtained for the decrease in various fractional derivatives and the assessment of $\omega = 50$ forcing angular frequency, which describes how that mode oscillates in time and controls how rapidly the external load changes in time at $x = 0.2$

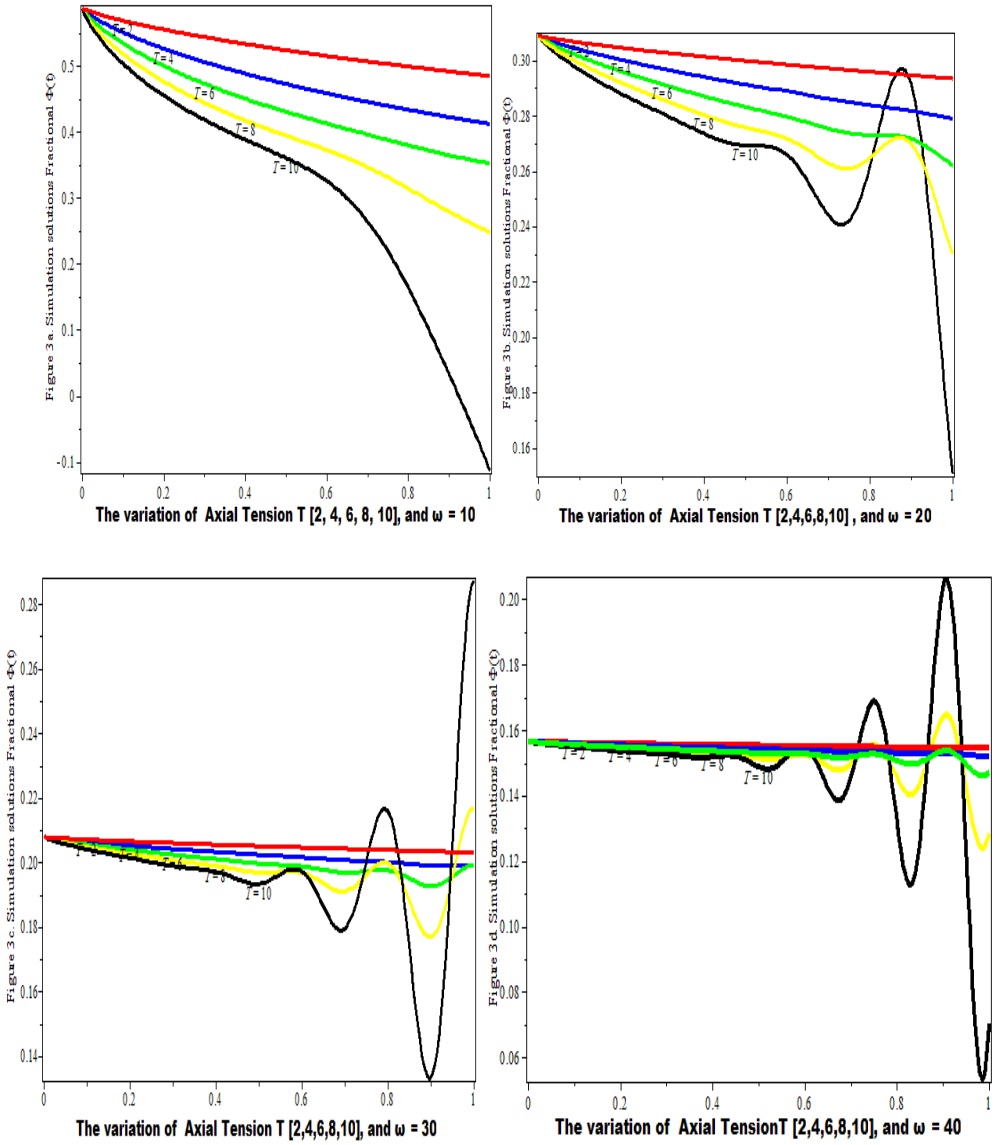

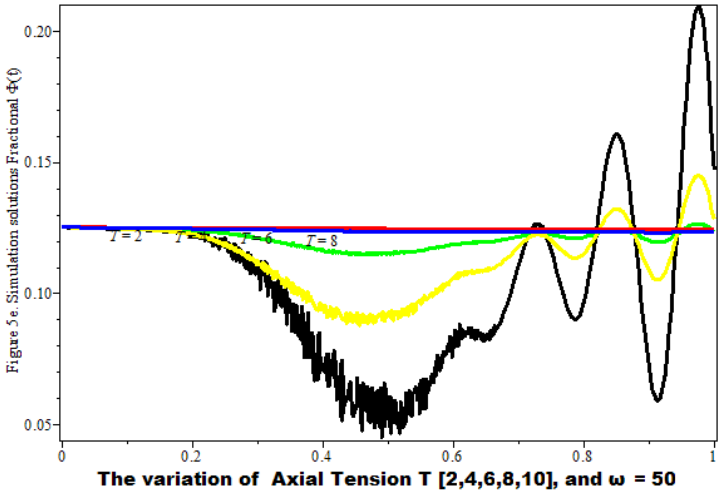

Fig. 3a.3b, 3c, 3d, 3e. depict the trend of the deflection $\Phi(t)$ obtained for the various of the axial tension $T = [2, 4, 6, 8, 10]$ when $\omega = [10, 20, 30, 40, 50]$ forcing angular frequency.

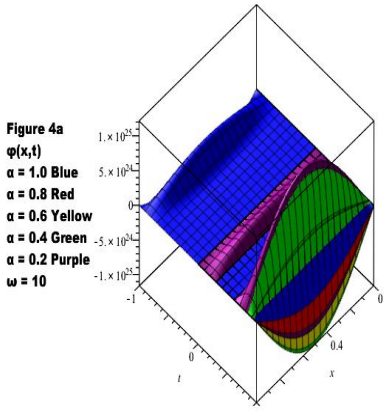

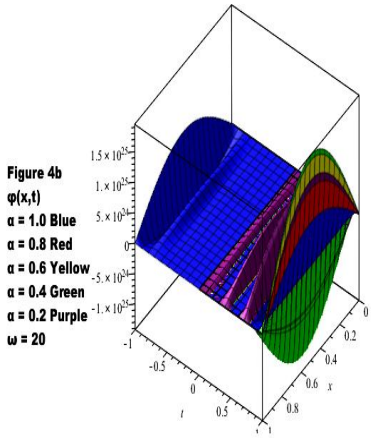

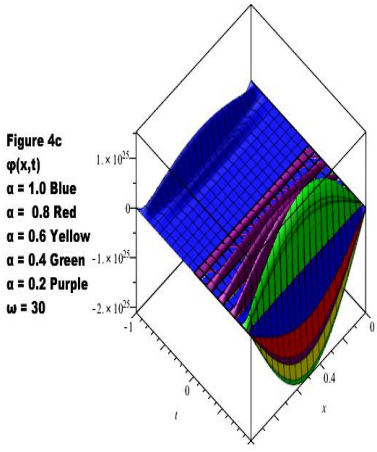

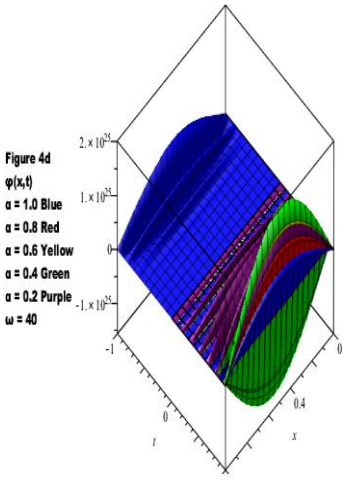

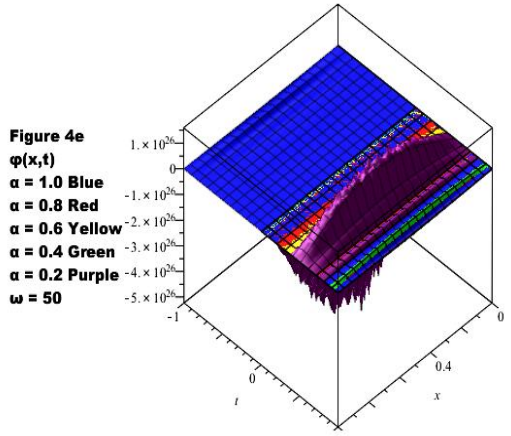

Fig. 4a.4b, 4c, 4d, 4e. Demonstrated the comparison of the deflection $\Phi(x,t)$obtained for the integer and fractional derivatives $\alpha = [1.0, 0.8, 0.6, 0.4, 0.2]$ of the vibration equation (1) with various $\omega = [10, 20, 30, 40, 50]$ forcing angular frequency.

Results and Discussion

Figure 1a: Depict the lower fractional order α yields higher vibration amplitudes and delayed damping, while higher α ensures quicker attenuation, **Figure 1b:** Demostrated the increasing α reduces oscillation amplitudes and accelerates damping, while smaller α sustains energy and oscillations, **Figure 1c: Indicated the** fractional damping governs energy dissipation; smaller α prolongs decay, whereas higher α suppresses vibrations efficiently and **Figure 1d:** Larger α values enhance damping and energy loss, while smaller α produce stronger, persistent oscillations.

ii. Figure 2a: Higher α values (0.8-1.0) stabilize oscillations, while lower α (0.2-0.4) cause unstable fluctuations. Figure 2b: Decreasing α intensifies negative response depth and instability; higher α yields smoother, shallower oscillatory behavior. Figure 2c: As α increases from 0.002 to 0.01, oscillation amplitudes decrease, and system stability improves. Figure 2d: Increasing α from 0.0002 to 0.001 reduces initial oscillations and promotes faster, smoother stability.

iii. **Figure 3a:** Increasing axial tension enhances stiffness, raises natural frequency, and reduces deformation amplitude for stable vibrations. **Figure 3b:** Higher tension accelerates decay, amplifies oscillations, and decreases system stability under constant forcing frequency. **Figure 3c:** Combined higher tension and frequency intensify oscillations, accelerate fluctuations, and magnify dynamic instability effects. **Figure 3d:** Increased

tension and forcing frequency amplify wave effects, producing stronger oscillations and higher instability.

iv. **Figure 4a:** Maximum deflection occurs at ω=10 for α=1.0; lower α values cause stronger damping. **Figure 4b:** At ω =20, higher α yields sharper oscillations, while smaller α shows greater damping effects. **Figure 4c:** Deflection decreases with smaller α; at ω =30, higher α maintains stronger vibration amplitudes. **Figure 4d:** Peak deflection at ω =40 for α α =1.0; smaller α values indicate enhanced damping effects and **figure 4e:** At ω = 50, α =1.0 shows highest amplitude; lower α reveals strong damping and memory effects.

Conclusion

This paper presents computational framework for solving the time-fractional vibration equation incorporating axial tension (T), flexural stiffness (R), and distributed load q(x,t) using a predictor-corrector algorithm. The results revealed that fractional-order derivatives effectively capture memory-dependent responses and nonlocal viscoelastic properties, improving the classical vibration theory for beams and cables under dynamic loading. Figures 1a-1d demonstrated that the fractional order α strongly influences damping and energy dissipation: lower α values prolong oscillations with larger amplitudes, while higher α ensures faster decay and enhanced stability. Figures 2a-2d confirmed that increasing α stabilizes the system, reduces oscillatory depth, and improves smoothness, whereas smaller α induces instability and deeper vibration troughs. Figures 3a–3d illustrated that axial tension T enhances stiffness and natural frequencies, reducing deformation amplitude and stabilizing vibration responses, though excessive tension can increase dynamic instability at higher forcing frequencies. Figures 4a–4e showed that higher fractional orders yield stronger but rapidly damped oscillations, while lower orders exhibit increased damping and memory effects, emphasizing the nonlocal nature of fractional systems.

Overall, the study confirmed that fractional-order modeling provides a more accurate and flexible approach for simulating vibration behavior in structural systems. The proposed predictor-corrector algorithm efficiently captures the complex interplay between fractional damping, tension, stiffness, and external excitation, making it a valuable computational tool for understanding and controlling vibration in mechanical and structural engineering applications.

References

[1] Srivastava, H. M., Kumar, D., & Singh, J. (2017). An efficient analytical technique for fractional model of vibration equation. *Applied Mathematical Modelling, 45*, 192–204. https://doi.org/10.1016/j.apm.2016.12.008

[2] Singh, H. (2018). Approximate solution of fractional vibration equation using Jacobi polynomials. *Applied Mathematics and Computation, 317*, 85–100. https://doi.org/10.1016/j.amc.2017.08.057

[3] Jena, R. M., & Chakraverty, S. (2019). Residual power series method for solving time-fractional model of vibration equation of large membranes. *Journal of Applied and Computational Mechanics, 5*(4), 603–615. https://doi.org/10.22055/jacm.2018.26668.1347

[4] Abro, K. A., & Yıldırım, A. (2019). Fractional treatment of vibration equation through modern analogy of fractional differentiations using integral transforms. *Iranian Journal of Science and Technology, Transactions A: Science, 43*, 2307–2314. https://doi.org/10.1007/s40995-019-00687-4

[5] Akshey, A., & Singh, T. R. (2024). A novel analytical iterative approach to time-fractional vibration equation using Aboodh transform. *Physica Scripta, 100*(1), Article 015296. https://doi.org/10.1088/1402-4896/ad9e4c

[6] Kasimala, N., & Chakraverty, S. (2024). Vibration equation of large membranes in uncertain environment. *Journal of Vibration Engineering & Technologies*. Advance online publication. https://doi.org/10.1007/s42417-024-01411-2

[7] Aghchi, S., Sun, H., & Fazli, H. (2024). Operational matrix approach for solving fractional vibration equation of large membranes with error estimation. *Filomat, 38*(6), 2205–2216. https://doi.org/10.2298/FIL2406205A

[8] Aghchi, S., Fazli, H., & Sun, H. (2024). A numerical approach for solving optimal control problem of fractional order vibration equation of large membranes. *Computers & Mathematics with Applications, 165*, 19–27.

[9] Ji, M., Wu, L., Liu, C., He, Y., & Qiao, Z. (2025). Time-delay fractional vibration resonance boosted weak fault detection of machinery. *Journal of Physics: Conference Series, 2999*(1), 012058.

[10] Łabędzki, P. (2025). Fractional Kelvin–Voigt model for beam vibrations: Numerical simulations and approximation using a classical model. *Electronics, 14*(10), Article 1918. https://doi.org/10.3390/electronics14101918

[11] Jafari, K., Rouzegar, J., Heydari, M. H., & Hosseininia, M. (2025). A cardinal-based approximate method for time fractional forced vibration analysis of Euler–Bernoulli viscoelastic beam. *Mathematical Methods in the Applied Sciences, 48*(9), 10046–10058. https://doi.org/10.1002/mma.10866

[12] Ullah, S., Zhong, Y., & Zhang, J. (2019). Analytical buckling solutions of rectangular thin plates by straightforward generalized integral transform method. *International Journal of Mechanical Sciences, 152*, 535–544. https://doi.org/10.1016/j.ijmecsci.2019.01.025

[13] Miller, K. S., & Ross, B. (2023). *An introduction to the fractional calculus and fractional differential equations*. John Wiley & Sons.